JOURNAL OF MATERIALS SCIENCE 28 (1993) 193–202

Friction and wear of P/M Al–20Si–Al_2O_3 composites in Kerosene

J. DUSZCZYK, D. BIALO*
Laboratory for Materials Science, Delft University of Technology, Rotterdamseweg 137, 2628 AL Delft, The Netherlands

The results of friction and wear of powder metallurgy (P/M) Al–20 wt% Si–3 wt% Cu –1 wt% Mg–(2.5–10) vol% Al_2O_3 particulate-reinforced composites have been compared with those of the P/M aluminium alloy matrix and A-390 cast piston aluminium alloy. It was found that Al_2O_3 reinforcement reduces wear by five to eight times when mating with cast iron in kerosene: The higher the reinforcement volume, the lower was the wear. With increased volume of reinforcement the wear mechanism of composites changed from the adhesive to the fatigue/delaminating one. The wear of the cast-iron counter sample was several times higher than that for P/M composites. Considering the life of the piston–piston ring couple, the piston composite with 10 vol% Al_2O_3 appears to be the best. The rate of clearance development for this couple is twice as low as that for the conventional piston alloys.

1. Introduction

Work on the development of improved internal combustion engines is currently being carried out in many research centres. Ever increasing requirements are specified for performance parameters such as higher cylinder pressures and operating temperatures. Also specified are life and reliability requirements. In addition, extensive care for the protection of the environment nowadays calls for more and more severe requirements related to fuel combustion, noise and gas emissions and lubricating oil consumption [1]. An essential provision for meeting these requirements is to develop better engine materials.

Pistons, manufactured conventionally from aluminium castings, are identified as the weakest components [1] of the engine. Therefore attempts are made to introduce new materials, which involve the application of modern manufacturing processes, for example, squeeze casting [2, 3] or powder metallurgy [4].

It is hoped, that the introduction of powder metallurgy (P/M)-produced alloys will provide an excellent basis for the production of engine pistons, able to meet the high requirements [5]. These materials demonstrate a much higher strength than those of conventional alloys, both at ambient and at elevated temperatures. They show a homogeneous, fine microstructure, which provides better tribological properties [5–7].

The outstanding feature of these materials is that their composition can easily be modified. Two approaches are usually supplied. In the first case, during the atomization process, alloying elements such as iron and nickel [8, 9] form hard, intermetallic phases, uniformly dispersed in the matrix. In the second case, matrices can be reinforced with ceramic particles (Al_2O_3, SiC, Si_3N_4, SiO_2, TiC, TiB_2) [3, 6, 10], whiskers or fibres [11–13].

The main objective of this work was to determine the effect of hard particulate Al_2O_3 reinforcement on the tribological properties of the material under conditions which simulate the piston performance. In particular, efforts were made to simulate the operating conditions of a piston mating with cast-iron piston rings.

During each work cycle of the engine, the piston moves not only axially, but also radially. The amplitude of this movement depends on the clearance between the piston and the cylinder bore. When the piston moves across the cylinder bore, it also moves with respect to the piston rings, which continuously remain in contact with the cylinder wall. This relative movement of piston rings against piston ring grooves is performed under considerable pressures exerted by combustion gases, which usually leads to wear of the piston ring groove and, in consequence, to a leaky piston–ring–cylinder system. Therefore, the oscillating movement of specimens (piston material) against a counter specimen made of cast iron (piston ring) has been chosen in our study to simulate the wear performance of a piston.

2. Experimental procedure

The character of the test is shown in Fig. 1. Three specimens, 1, of the material to be characterized, are loaded with a conically shaped, cast-iron counter specimen, 2. This counter specimen is set to oscillating–rotary motions of a pre-set amplitude, A_m,

* *Permanent address*: Department of Precision Engineering, Warsaw University of Technology, Poland.

0022–2461

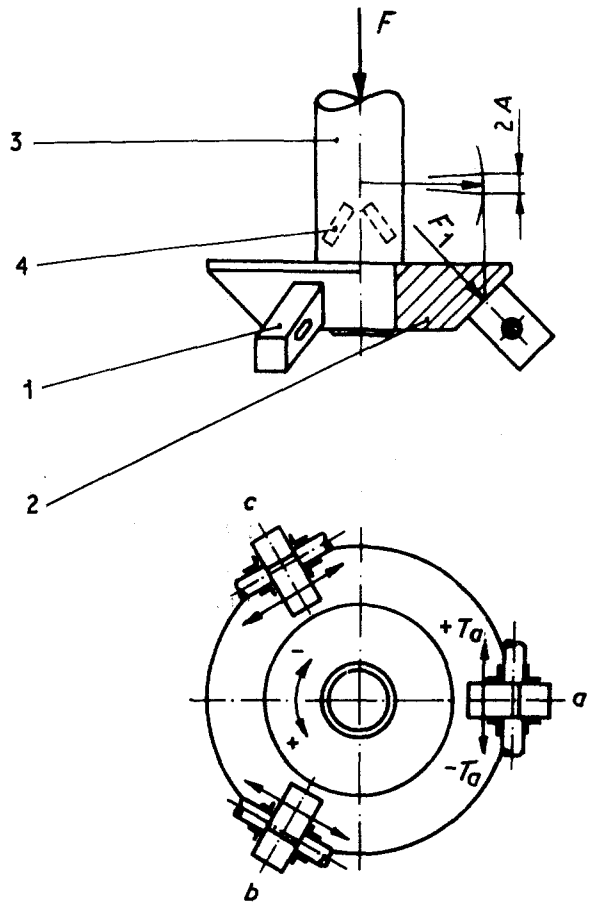

Figure 1 Specimens and counter specimen assembly.

measured in the middle of the area of friction of a specimen. Initially, the contact between the conical surface of the counter specimen and the flat surface of the specimen, results in line contact with high initial contact pressures.

The contact area increases rather rapidly, with contact pressure decreasing, respectively, until nominal pressure, P_N, at the contact area equal to the face area $a \times b$ of the specimen, is attained. The three specimens are placed concentrically against the conically shaped counter specimen in the axes providing for their correct adherence.

The vertical shaft 3, which exerts the load on the counter specimen, is set to an oscillating–rotary motion via a special eccentric (not shown in Fig. 1). In addition, the shaft is fitted with resistance strain gauges for the measurement of the friction force, T, between the counter specimen and the specimens.

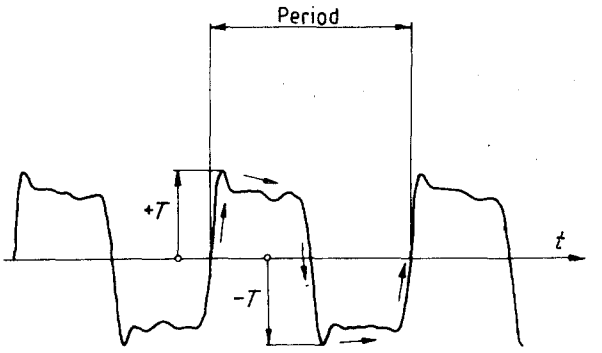

Figure 2 Friction force between specimens and counter specimen versus time.

A detailed description of the testing apparatus, complete with measuring and registering instruments, was presented earlier [7].

Typical changes in friction force versus time are plotted in Fig. 2. During one cycle, the force changes from $+T$ to $-T$. The tests were carried out under the following conditions: force acting on specimen, F_1, 74 N; contact pressure, F_1/ab, 3 MPa; amplitude, A_m, 352 μm; frequency, $33\,s^{-1}$; cycles, N, variable from $0.5–7 \times 10^6$; environment, kerosene. The tests were carried out at a temperature of 21 °C, in a kerosene environment, with the results being considered as preliminary and informative.

Kerosene was used as a protective medium to prevent oxidation of the specimen–counter specimen surfaces, because, as was found in our investigations [6], the Al–Si–X matrix composite materials will develop a thick oxide layer in an oxidizing environment. The oxides are easily removed during sliding and result in high rates of wear of the specimens. Future tests will be carried out under conditions very closely simulating the actual environment, including the temperature corresponding to that of the piston area in the vicinity of the piston groove, and an atmosphere similar to the composition of exhaust gases.

3. Materials and processing

The specification of the materials involved and their processing is given in Table I. Material A is a conventional cast piston alloy A-390 with an average silicon crystal size of 70 μm. The composition of material C is modified, taking advantage of the rapid solidification process which results in a very fine microstructure with fine silicon crystals of 5 μm. Powder C (average

TABLE I Composition and hardness of the specimen materials

Code	Hardness (HRB)	Composition (wt %, reinforcement vol %)	Processing
A	70.3	A390	Casting, T-6
C	77.1	ASCM	Extrusion, T-6
DU1	81.8	ASCM + 2.5Al_2O_3	Extrusion, T-6
DU2	83.0	ASCM + 5Al_2O_3	Extrusion, T-6
DU3	88.1	ASCM + 10Al_2O_3	Extrusion, T-6
		A 390 Al + 17Si + 4.5Cu + 0.6Mg + 0.3Fe	ASCM Al + 20Si + 3Cu + 1Mg

particle size 20–30 μm) has been developed and produced by Showa Denko KK, Tokyo, using air atomization. The composite materials DU1, DU2 and DU3 have been produced by dry mixing of matrix powder C with 2.5, 5 and 10 vol % Al_2O_3 particulate reinforcement, respectively. Al_2O_3 reinforcement particles are of irregular shape with sharp edges with an average particle size of 6 μm. The processing of the

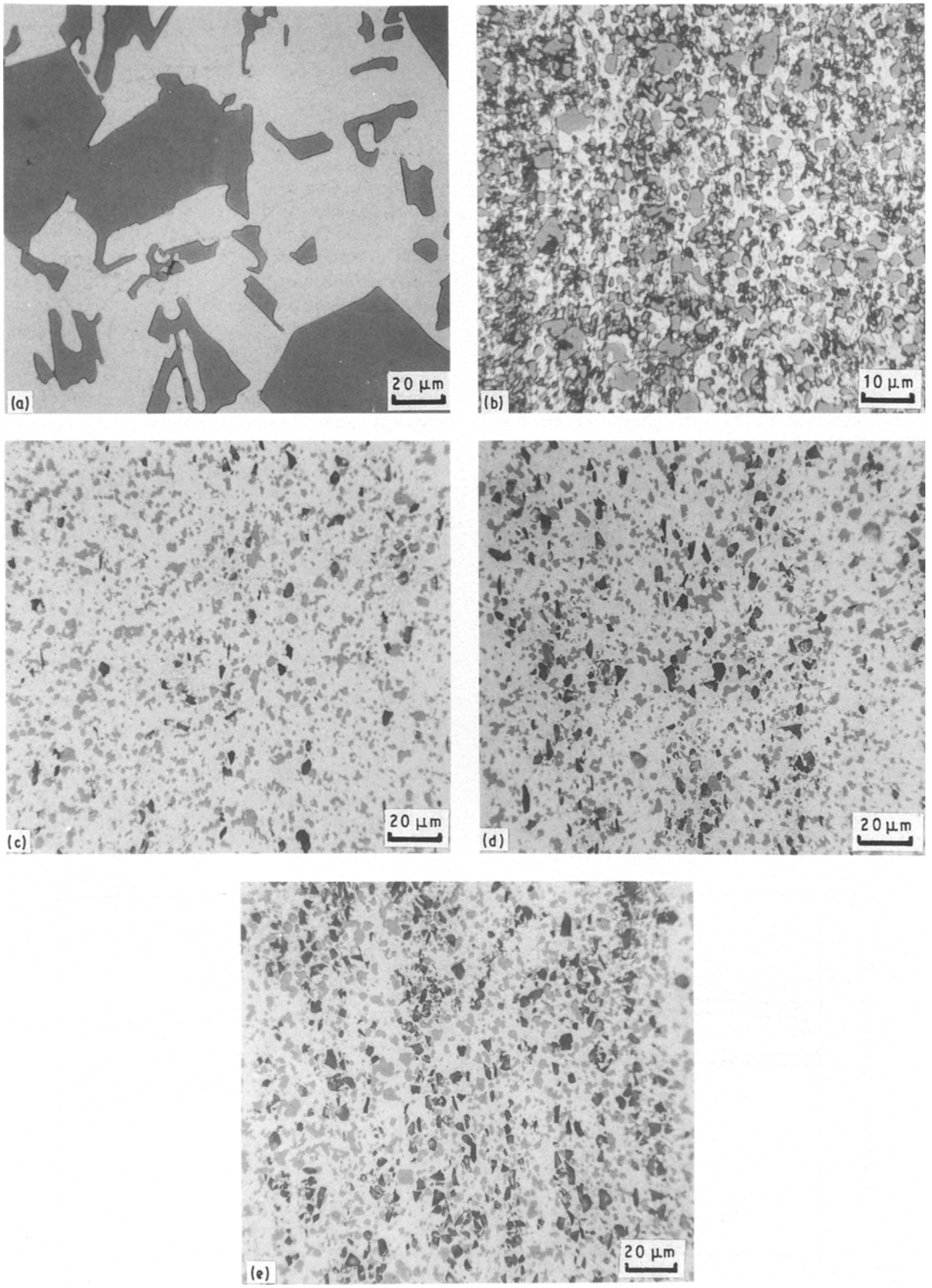

Figure 3 Microstructures of the materials after heat treatment. (a) Material A, (b) material C, (c) DU1 ($2.5Al_2O_3$), (d) DU2 ($5Al_2O_3$), (e) DU3 ($10Al_2O_3$).

P/M matrix and composites consisted of several steps: mixing (only for composites); precompaction combined with degassing; hot extrusion; and heat treatment. Extrusion was carried out on a 2 MN horizontal press with a reduction ratio of 20:1 using a graphite-based lubricant. The extrusion temperature was 370 °C.

The P/M materials could be extruded without difficulties, but cast material A could not be extruded, because of its inherent brittleness. Consequently, material A was used in the as-cast condition. All materials were heat treated by a T-6 temper treatment, which consisted of the following steps: solution heat treatment at 470 °C for 1.5 h; water quenching; ageing for 4 days at room temperature and then for 24 h at 120 °C.

Fig. 3 shows the microstructures of the materials after processing. Microstructures of P/M materials are taken in the longitudinal extrusion direction. The difference between the cast A390 piston alloy and the P/M matrix and composites is apparent. Material A is very coarse with large brittle silicon crystals. Silicon crystals in the P/M matrix are very fine and homogeneously dispersed. In the composites DU1, DU2 and DU3, Al_2O_3 particles (black colour) are homogeneously distributed and aligned in the longitudinal extrusion direction.

Silicon crystals (grey colour) are slightly finer in the P/M composites than those in the P/M matrix (C). This indicates that the P/M matrix without reinforcement is more susceptible to coarsening.

The differences in hardness (Table I) between the materials involved, can be explained by their microstructures. Finer silicon crystals and a higher volume of ceramic reinforcement increase the hardness.

All samples were prepared for subsequent wear tests in such a way that the friction force was transverse to the extrusion direction.

The cone-shaped counter specimens (Fig. 1) were made from cast iron of the following composition (wt %): C 3.4; Si 1.9; Mn 0.6; S 0.1; P 0.3; Ni 0.1; Cr 0.1; Fe remainder. The hardness of the counter specimens ranged from 190–198 HB.

4. Results and discussion

Fig. 4 shows the selected results of the average coefficient of friction versus the number of cycles for four materials. The curve for material DU2 (omitted in Fig. 4) is located between curves DU1 and DU3. The value of the average coefficient of friction, μ, was described as the quotient of the total friction force $T = (T_a + T_b + T_c)$ and $3F_1$ (as referred to in Figs 1 and 2).

It can be seen from Fig. 4, that the coefficient of friction changes rapidly during the initial period of friction. This period is characterized by the highest contact pressures between the specimens and the counter specimen due to the linear nature of contact. Low values of the coefficient of friction during the very initial period of wear tests are also reported for aluminium alloys by other authors [14, 15]. It is believed this phenomenon is the result of the presence of hard aluminium oxides at the friction interface, which are poorly bound to the substrate. We share this opinion. The particles of the crushed oxide layer are driven into surfaces of the specimen–counter specimen couple during the run-in period of the test working as solid lubricant. Then, as the number of cycles of the relative specimen–counter specimen movement increases, these particles are removed beyond the contact area, together with wear products. Only then does the friction mechanism start to change, which is indicated by a reduction of the coefficient of friction. For materials A and C this is connected with a change of the wear mechanism from adhesive–abrasive to adhesive. In the case of materials DU, the coefficient of friction takes higher values, which should be related to the presence of the hard Al_2O_3 particles with sharp edges. As the surface wears down, new hard particles are exposed. During this stage the counter specimen surface can be expected to be micromachined or

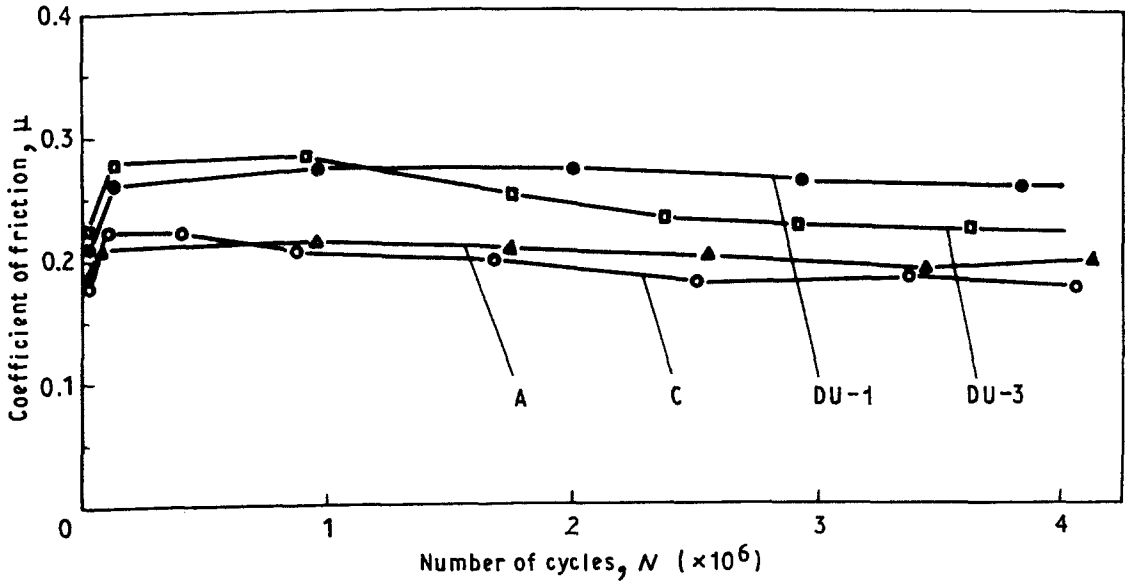

Figure 4 Average coefficient of friction versus number of cycles for materials A, C, DU1 ($2.5Al_2O_3$) and DU3 ($10Al_2O_3$).

ploughed. From this point of view, the sequence of the DU curves is somewhat surprising. It was expected that the highest volume of Al_2O_3 (material DU3) would provide the highest coefficient of friction. The values of the coefficient of friction, related to particular materials and shown in Fig. 4, tend to stabilize after a considerable number of cycles (approximately 2.5×10^6). Fig. 5 shows the wear results as the mass loss of the specimens versus number of cycles.

It can be seen that the highest wear rate is found with the conventional cast alloy A. With material C of similar composition but produced by powder metallurgy methods, a higher resistance to wear has been attained. This should be related to the fine structure and higher hardness of material C. However, the essential change of wear resistance reaching levels that are several times higher, has been attained only with the composite materials.

It is believed that for the results presented in Figs 4 and 5, none of the simple correlations between friction and wear, as usually observed in tribological investigations, can be applied. Thus, the materials DU showing higher coefficients of friction when mating with cast iron than those shown by the materials A and C, wear several times slower. This can only indicate that it is not the tribological, but the compositional structure characteristic of the materials that is decisive for the wear rates under the present test conditions, i.e. in kerosene. It should be added that the tests carried out with the same materials and under similar load and kinematic conditions [6], but in an oxidizing atmosphere (air at 21 °C), have yielded entirely different results. Under oxidizing wear conditions, the weight losses of the specimens were as much as 20 times higher, but the values of the mass loss, ΔM, varied only very slightly from one material to another.

The results of the wear tests, shown in Fig. 5, are used to calculate specific wear rates, w.

$$w = \frac{\Delta V}{F_1 \Delta s} \text{mm}^3 \text{N}^{-1} \text{m}^{-1} \quad (1)$$

where ΔV is the volume of removed materials (mm^3) at Δs, Δs the length of friction distance (m), and F_1 the normal force of the specimen against the counter specimen. The value of the friction distance, $\Delta s = 1408$ m, which corresponds to 1×10^6 cycles of relative motion against the counter specimen (distance covered during one cycle, was 4 $A_m = 1.408$ mm), is applied in the calculations.

Fig. 6 presents the values of the specific wear rates, w, for the materials investigated. It can be seen that the materials investigated show the highest specific wear rate during the run-in period. This particularly applies to the relatively softer materials A and C, with the respective values amounting to 1.6 and 1.2 $\times 10^{-6}$ $\text{mm}^3 \text{N}^{-1} \text{m}^{-1}$. With an increasing number of cycles, specific wear rates for the materials A and C decrease significantly, reaching the values 0.6×10^{-6}–0.7×10^{-6} $\text{mm}^3 \text{N}^{-1} \text{m}^{-1}$ at 7×10^6 cycles. With the materials DU, the specific wear rate, w, is several times lower than with A and C; and the variations from one value to another within the range 1×10^6–7×10^6 cycles are smaller.

An attempt has also been made to determine the correlation between the wear rate and hardness of the materials involved. As can be seen from Fig. 7, such a correlation exists, i.e. the lower wear rates correspond to higher hardness values. However, the results of the

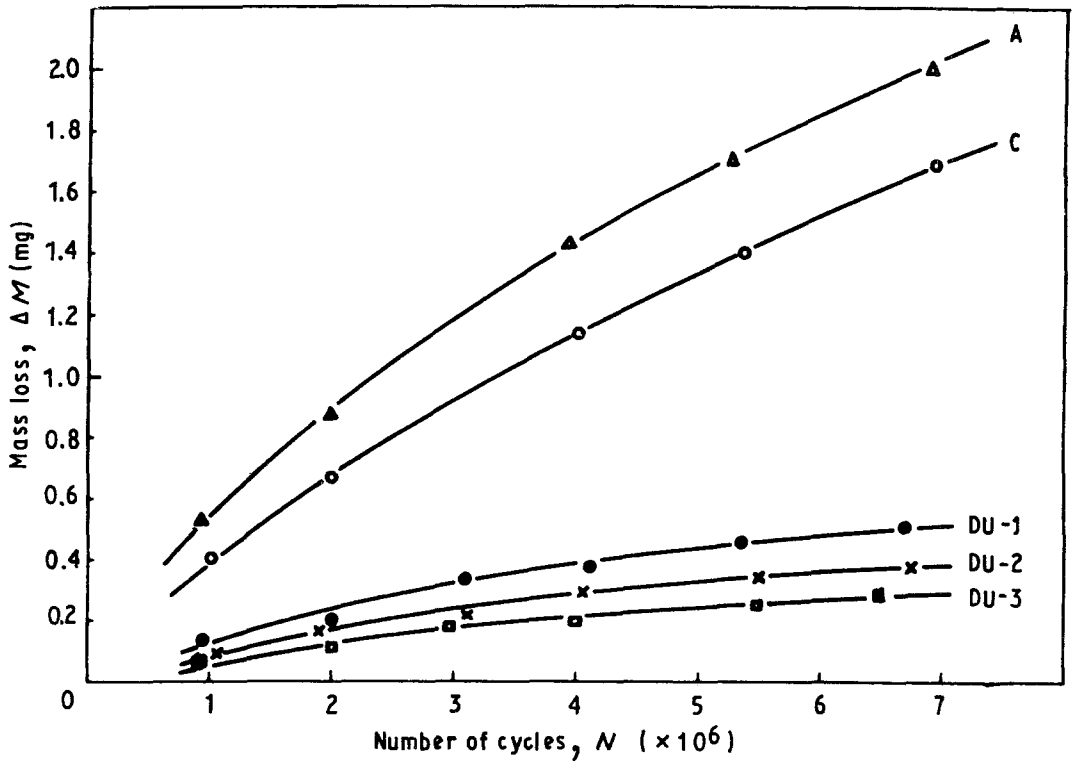

Figure 5 Mass loss of the specimens versus number of cycles.

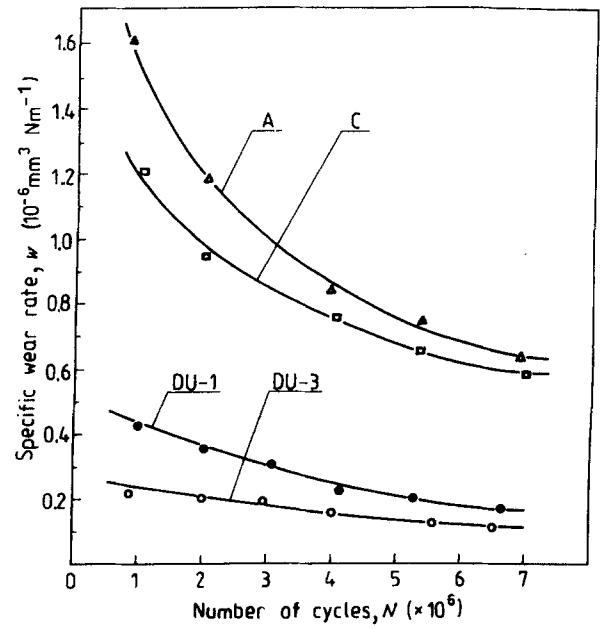

Figure 6 Specific wear rate of the materials as a function of the number of cycles.

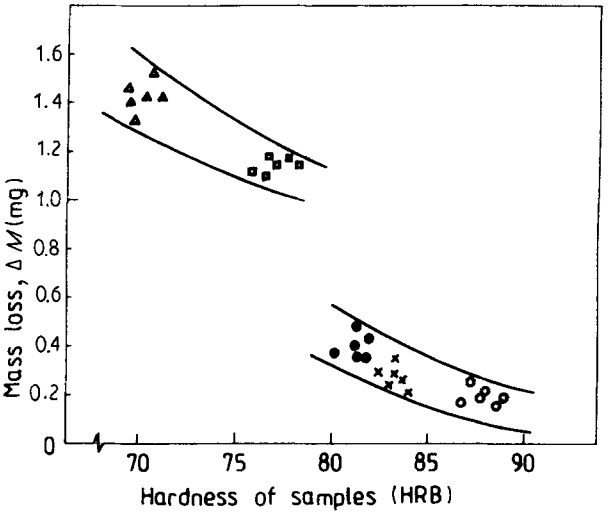

Figure 7 Correlation between mass loss and hardness of the specimens (ΔM after 4×10^6 cycles). Materials: (△) A, (□) C, (●) DU1, (×) DU2, (○) DU3.

tests must be divided for two groups of materials. One of these concerns the structurally similar materials A and C, while the other group concerns the composite materials.

It is essential for tribological investigations that the wear rates of both partners of the friction couple should be considered. There may be cases where the wear rate of the counter specimen could have a stronger impact on the mating of cooperating components, including the development of leakages and clearances, etc., than that of the specimen itself. Unfortunately, this factor is very seldom reported in the literature. In the present work, volumetric wear of the specimens was determined with Talyrond 200 equipment by recording their roundness errors. The graph was made from the recorded section area of the worn surface and the wear trace volume was calculated.

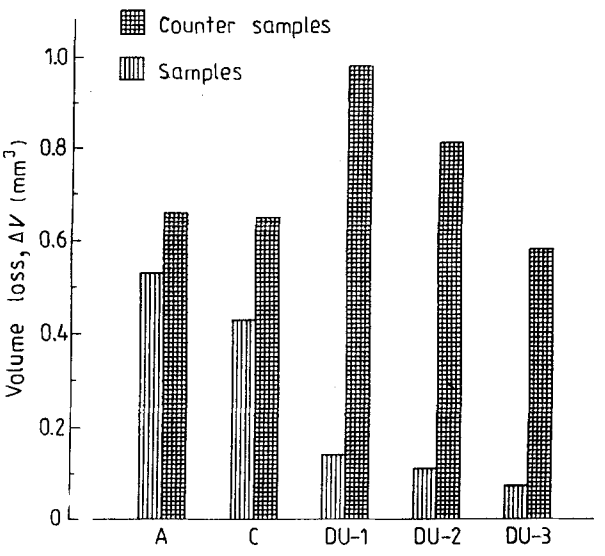

Figure 8 Volume loss of the specimens and of the cast-iron counter specimens after 4×10^6 cycles.

In Fig. 8 the results of the wear rate of the specimens are shown compared with those of the relative counter specimens. The results are surprising, because the wear rate of the cast-iron counter specimens is always higher than that of the specimens themselves. We admit that we did expect different relations, especially for materials A and C, which were much softer than the iron counter specimens (Table I). The wear rate of the counter specimens was several times higher than that of the DU specimens. Presumably, the wear surface of the specimens acted on the counter specimens similar to a grinding wheel with abrasive Al_2O_3 particles. The higher the content of Al_2O_3 particles, the lower the wear rate of the DU specimen and also the lower the wear rate of the cast-iron counter specimen. This can be explained by the fact that with a higher volume of Al_2O_3, the composite matrix becomes stronger and harder. Therefore, it will wear at a lower rate. Moreover, it will expose new ceramic particles at a slower rate, causing lower wear rate of the counter sample.

Table II presents the linear wear of the specimens and counter specimens after completing 4×10^6 cycles. Wear of the specimens, δ_1, was calculated from the

TABLE II Linear wear, δ, of the specimens and counter specimens after 4×10^6 cycles

	Specimen and counter specimen material				
	A–cast iron	C–cast iron	DU1–cast iron	DU2–cast iron	DU3–cast iron
Wear of the specimens, δ_1 (μm)	22.1	17.9	5.8	4.6	3.1
Wear of the counter specimens, δ_2 (μm)	27.5	27.1	40.8	33.8	24.2
Total wear, δ (μm)	49.6	45.0	46.6	38.4	27.3

wear volume losses, but the linear wear of the counter specimens was assumed as the average depth of the wear trace as measured with the Talyrond 200 instrument. The total wear $\delta = \delta_1 + \delta_2$ describes the distance of the displacement of the specimen against the counter specimen during the test; δ can be interpreted as a parameter equivalent to the index of development of clearance between mating parts. The value of the total wear, δ, was the highest for the material couple A–cast iron. Respective values for the material couples

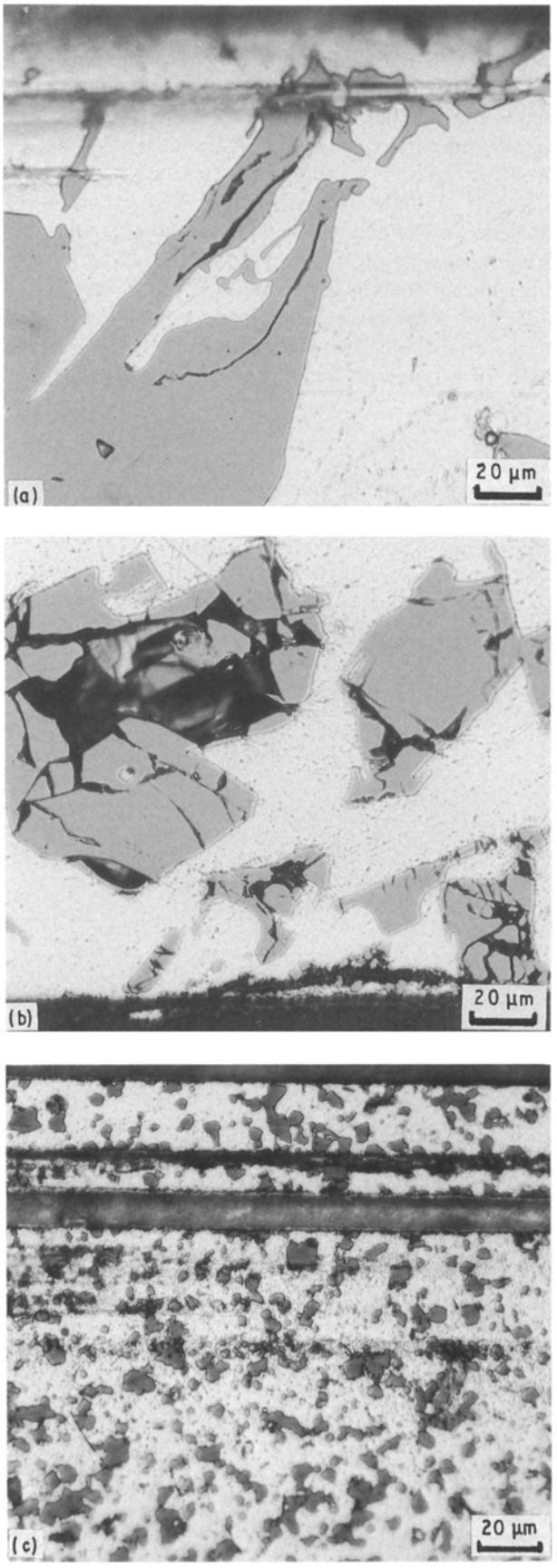

Figure 9 Subsurface microstructures in the plane parallel to the direction of movement of materials (a, b) A and (c) C (oblique sectioning at 6°).

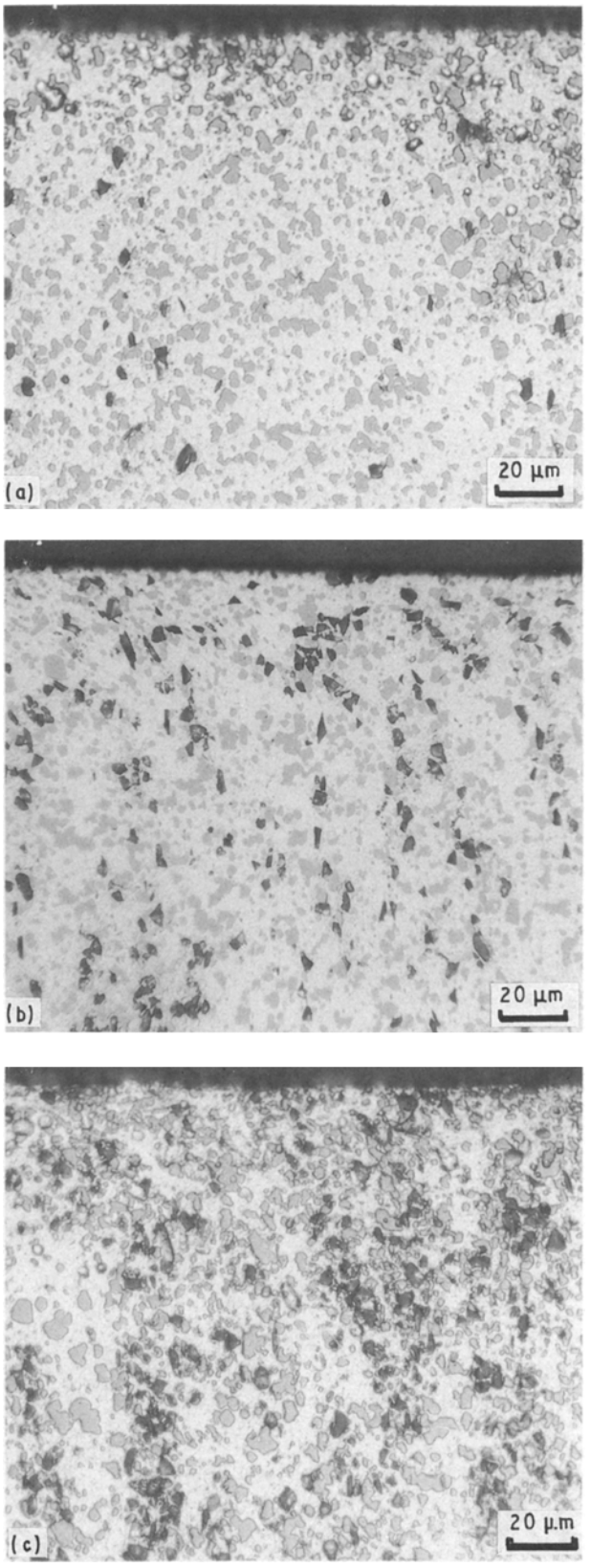

Figure 10 Subsurface microstructures in the plane parallel to the direction of movement of materials (a) DU1, (b) DU2 and (c) DU3 (oblique sectioning at 12°).

DU1–cast iron and C–cast iron were not much lower. Significant improvement was attained with the materials DU2 ($5Al_2O_3$) and, in particular, with the couple DU3 ($10Al_2O_3$)–cast iron.

Figs 9 and 10 show subsurface microstructures in the vicinity of the wear area for all the test materials. The microsections were made in a plane parallel to the direction of friction, at an angle 6° and 12° against the friction surface. Material A shows broken silicon crystals, which weaken the subsurface structure. As the wearing of the surface proceeds, these particles are removed together with the wear products. This phenomenon could be responsible for the relatively higher wear rate of material A. It is worth noting that under a higher load (129 N) significant plastic deformation combined with a reduction in silicon size is observed in material A up to a depth of 10 μm. No significant changes can be observed in the subsurface microstructure of material C. Dispersed silicon particles can be seen only very close to the worn surface, as a consequence of the direct contact when mating with the counter specimen. Similar observations relate to the materials DU.

Fig. 11 shows the morphology of worn surfaces of materials A and C. The photograph (Fig. 11a) shows a section of the surface containing a silicon crystal. It can be seen that a number of crystal fragments have already been released from the matrix and will soon be removed, together with the other wear products. The remaining part of the crystal is bound to the matrix. Another section of the same surface is shown in Fig. 11b at higher magnification. Two wear mechanisms can be distinguished: ploughing and adhesion. Fine, flaky wear products, of sizes below a fraction of a micrometre, become separated from the surface due to adhesion. A similar wear mechanism can be attributed to material C. Fig. 11d shows a picture of this material with two types of wear product. The smaller one

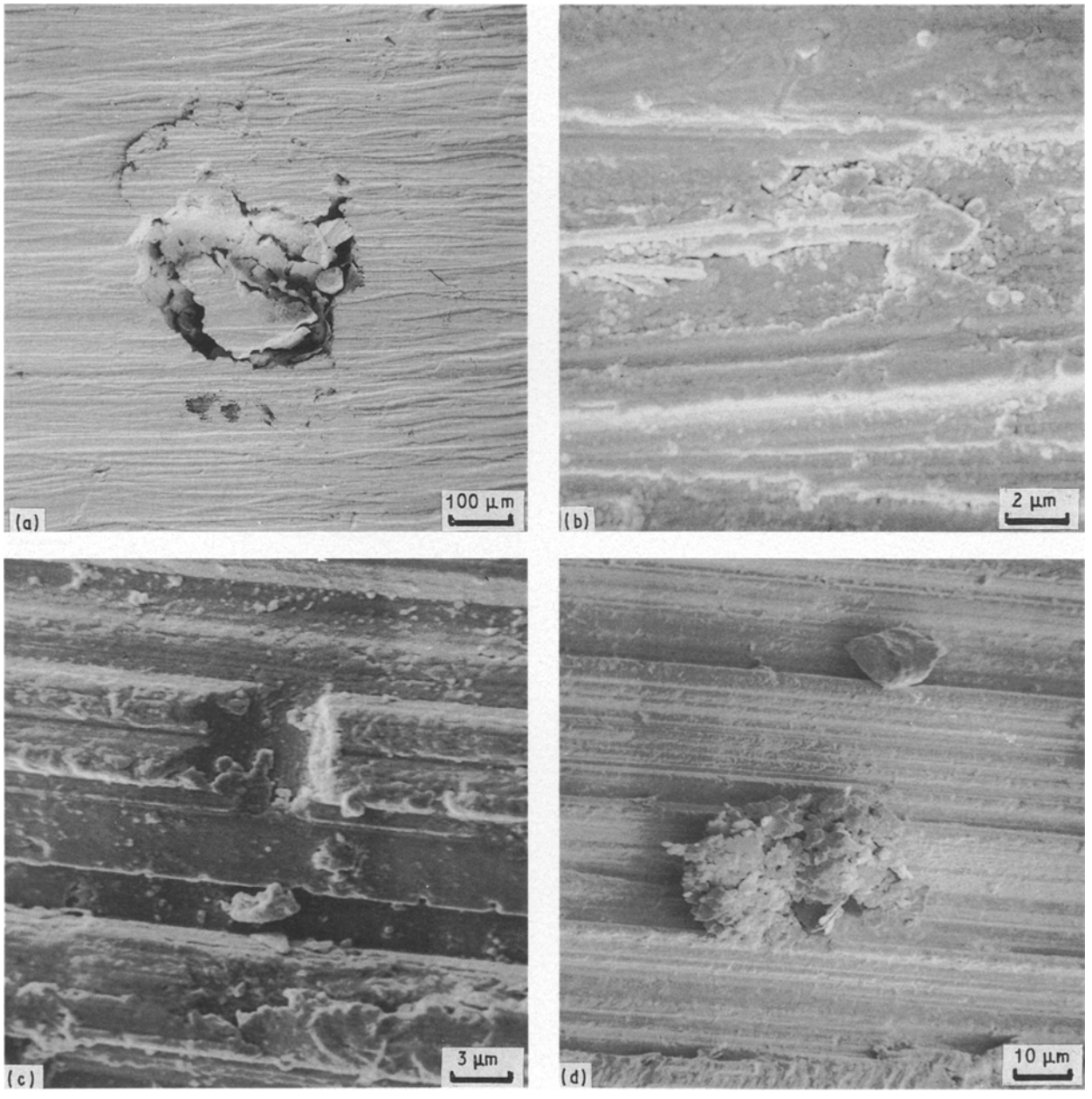

Figure 11 Scanning electron micrographs of worn surfaces of material (a, b) A and (c, d) C.

consists of silicon crystals and the second one of a conglomerate of very fine adhesive wear products. These products tend to take the shape of bodies of revolution, the sizes of which depend on the dimensions of the grooves they move along over the specimen and the counter specimen surfaces. They are not very durable and easily disintegrate during, for example, washing in a supersonic bath. Such wear products taking the shapes of bodies of revolution, e.g. rollers, were also observed by other authors [16]. However, the conclusion drawn by them, suggesting that these bodies separate two friction surfaces and therefore the friction is of the rolling type, seems questionable.

For DU materials the difference in morphology of worn surfaces is shown in Fig. 12. It is apparent that with increased reinforcement volume the surface of worn samples becomes less deformed and smoother. This is consistent with the position of the wear curves in Figs 5 and 8. Moreover, with increased reinforcement volume, the wear mechanism of composites changes from adhesive (DU1–2.5Al_2O_3, DU2–5Al_2O_3) to fatigue/delamination (DU3–10Al_2O_3). The fatigue mechanism can be distinguished through the development of cracks at the worn surface of the DU3 composite (Fig. 12d). The wear products of the DU3 composite are of laminar shape indicating the delaminating nature of the wear mechanism. This type of wear has already been reported in the literature [17].

6. Conclusions

An addition of Al_2O_3 particulate reinforcement to the P/M Al–20Si–X matrix reduces the wear of composites five to eight times during oscillating motions

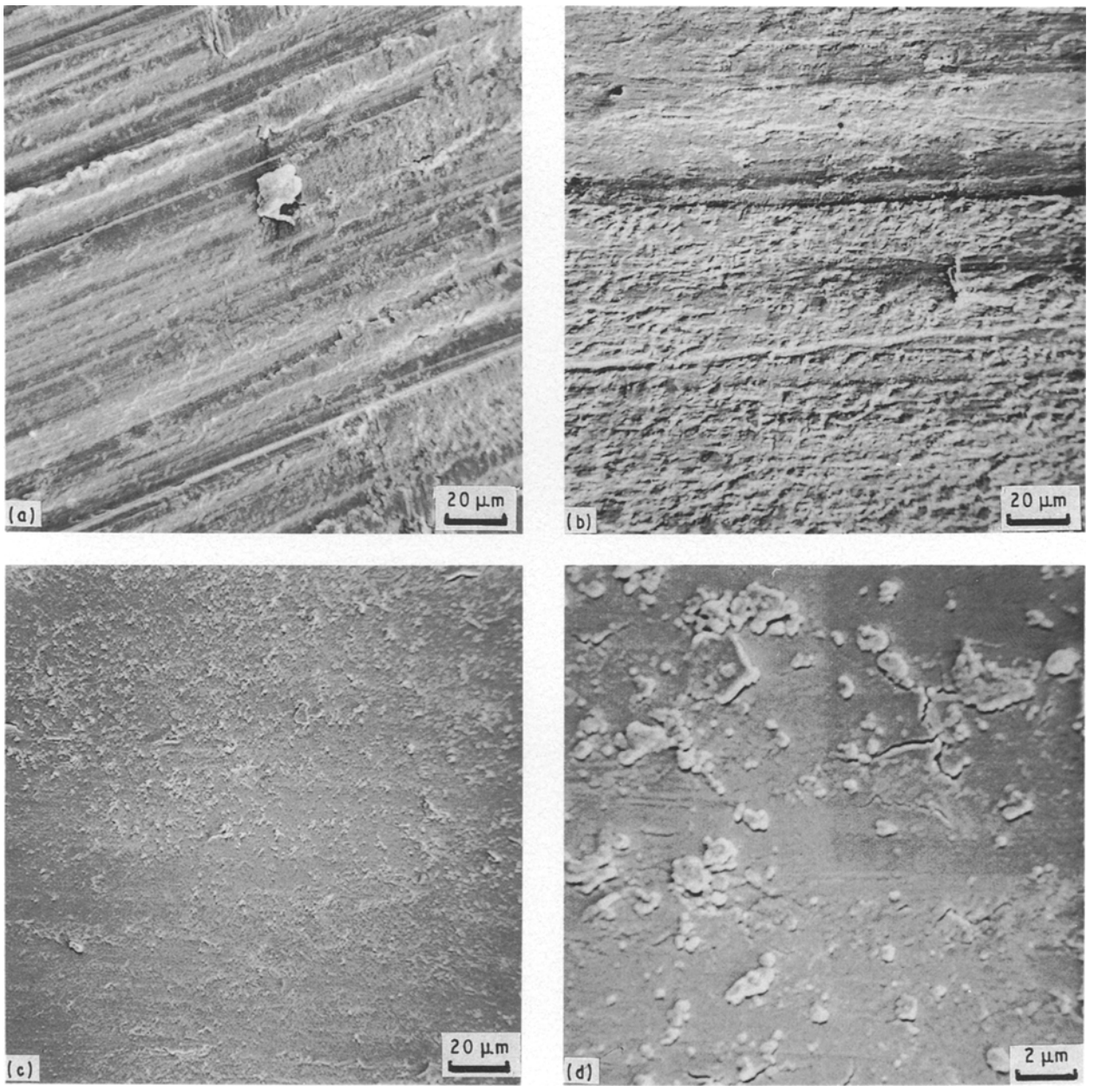

Figure 12 Scanning electron micrographs of worn surfaces of materials (a) DU1, (b) DU2, (c, d) DU3.

when mated with a cast-iron counter specimen in kerosene: the higher the reinforcement volume, the lower was the wear. With increased volume of reinforcement the wear mechanism changes from adhesion and ploughing (matrix, composites with 2.5 and $5Al_2O_3$) to fatigue and delamination (composite with $10Al_2O_3$). The wear of the cast iron counter sample is several times higher than that of the P/M composites. Moreover, it is higher for the composites worn by adhesion (DU1, DU2) than that for the A390 piston cast alloy and P/M Al–20Si–X matrix.

Therefore, considering the life of the piston–piston ring couple, the best composite is the piston composite with $10Al_2O_3$. The rate of clearance development for this couple is twice as low as that for the conventional piston alloys. No correlation between the wear rate and the coefficient of friction of the materials investigated has been found.

Acknowledgements

The authors are indebted to Professor Dr Ir B. M. Korevaar for stimulating discussions, Mr T. L. J. de Haan and Ing. E. J. A. van Dam for skillful assistance with the optical microscopy and SEM, Dr Ir G. J. J. van Heijningen and Professor Ir A. W. J. de Gee for providing the equipment for the wear tests. We are also much obliged to Ir H. Zitman and Ir J. Giesberts, Mifa Aluminium BV (Venlo), for valuable discussions on the processing of metal matrix composites. The financial support of the Foundation for Technological Research-STW and the Programme for Stimulation of Industrial Oriented Technologies (PBTS) is gratefully acknowledged. Powders were supplied by the Japanese firm Showa Denko.

References

1. R. R. BOWLES, D. L. MANZINI and M. W. TOAZ, in "Advanced Composites" (ASM International, Metal Park, OH, 1986) p. 21.
2. Y. M. PAN, H. S. CHENG and M. E. FINE, in "Fundamental relationship between microstructures and mechanical properties of metal matrix composites", edited by P. K. Liaw and M. N. Gungor (TMS, PA, 1990) p. 637.
3. G. CHADWICK and L. FROYEN (eds), "Metal Matrix Composites" (North-Holland, Amsterdam, 1991).
4. N. AMANO, Y. ODANI, Y. TAKEDA and K. AKACHI, *Metal Powder Rep.* **44** (1989) 186.
5. V. ARNHOLD and D. MÜLLER-SCHWELLING, Paper 910156 (SAE International, Warrendale, PA, 1991).
6. D. BIALO and J. DUSZCZYK, unpublished research, Delft University of Technology, The Netherlands.
7. D. BIALO, J. DUSZCZYK, A. W. J. de GEE, G. J. J. van HEIJNINGEN and B. M. KOREVAAR, *Wear* **141** (1991) 291.
8. J. ZHOU, J. DUSZCZYK and B. M. KOREVAAR, *J. Mater. Sci.* **26** (1991) 3041.
9. *Idem, ibid.* **27** (1992).
10. A. SATO and R. H. MEHRABIAN, *Metall. Trans. B* **7** (1976) 443.
11. J. H. ter HAAR and J. DUSZCZYK, *J. Mater. Sci.* **26** (1991) 3628.
12. T. NASHIMURA, L. THAN TRONG and M. KIKUCHI, in "Proceedings of the Japan Institute of Tribology Conference" (Japanese Society of Tribologists, Tokyo, November 1990) p. 677.
13. L. CAO, Y. WANG and C. K. YAO, *Wear* **140** (1990) 273.
14. C. CHIU, J. D. EMBURY and T. CASTILLO, *Metallography* **20** (1987) 99.
15. H. GOTO, M. ASHIDA and K. ENDO, *Wear* **116** (1987) 141.
16. A. A. SCHANYAVSKIJ, B. J. BUSTSEV and M. V. ISAEV, *Izviest. Akad. Nauk SSSR, Metally* **4** (1985) 136.
17. B. N. PRAMILA BAI and S. K. BISKWAS, *J. Amer. Soc. Lubric. Eng.* January (1987) 57.

Received 28 January
and accepted 17 February 1992